

REVIEWS OF TOPICAL PROBLEMS

PACS numbers: 95.55.Ka, 97.80.Gm, 98.70.Rz

Cosmic gamma-ray bursts and soft gamma-repeaters — observations and modeling of extreme astrophysical phenomena

(100th anniversary of the Ioffe Institute)

R L Aptekar, A M Bykov, S V Golenetskii, D D Frederiks, D S Svinkin, M V Ulanov, A E Tsvetkova, A V Kozlova, A L Lysenko

DOI: https://doi.org/10.3367/UFNe.2018.11.038488

Contents

Abstract. **Cosmic gamma-ray bursts (GRBs) and soft gamma-ray repeaters (SGRs) are the brightest sources of high-energy electromagnetic radiation. For many years, GRB and SGR studies have been among the major basic research areas at the Ioffe Institute. The physical processes that power immense luminosity of the cosmic gamma-ray sources are of utmost interest because they enable exploring physical phenomena in the vicinities of stellar-mass black holes and neutron stars, whose magnetic fields are probably larger than the critical vacuum polarization value, i.e., under conditions inaccessible in terrestrial laboratories. Owing to the high luminosity, GRBs can be detected at distances up to the edge of the visible Universe, and thus enable studying how the first stars emerged and probing the properties of matter along the entire line of sight to the sources. We briefly review the results of modern multi-wavelength studies of cosmic GRBs and SGRs. We discuss the history of the GRBs and SGRs studies, a vibrant area of basic astrophysical research at the Ioffe Institute, their accomplishments and prospects. We describe in detail the results obtained with several generations of KONUS detectors that have been designed and manufactured at the Ioffe Institute. Observational data obtained by space-based instruments are effectively complemented by theoretical modeling of astrophysical processes that exhibit extreme energy release. We also discuss prospects for GRB and SGR studies, including future experiments scheduled at the Ioffe Institute.**

R L Aptekar(*), **A M Bykov, S V Golenetskii, D D Frederiks, D S Svinkin, M V Ulanov, A E Tsvetkova, A V Kozlova, A L Lysenko**
Ioffe Institute, ul. Politekhnicheskaya 26, 194021 St. Petersburg, Russian Federation
E-mail: (*) aptekar@mail.ioffe.ru

Received 23 August 2018, revised 23 November 2018
Uspekhi Fizicheskikh Nauk **189** (8) 785 – 802 (2019)
DOI: https://doi.org/10.3367/UFNr.2018.11.038488
Translated by K A Postnov; edited by A M Semikhatov

Keywords: cosmic gamma-ray bursts, soft gamma repeaters, burst light curves, burst energy spectra

1. Discovery of cosmic gamma-ray bursts by American Vela satellites. First deep studies of the new phenomenon in KONUS experiments aboard Venera 11–14 interplanetary missions. BATSE experiment. KONUS–WIND experiment

Cosmic gamma-ray bursts (GRBs) were discovered by American Vela satellites that were launched into remote orbits around Earth with altitudes of about 100,000 km. The satellites were equipped with simple gamma-ray detectors to control the Partial Test Ban Treaty (PTBT). Coordinates of gamma-ray sources were calculated using the triangulation method from the propagation time delay of radiation between several satellites. Observations by Vela satellites were conducted from the mid-1960s to the end of the 1970s. No violations of the PTBT by signatory countries were found, but by the beginning of the 1970s, detectors aboard the Vela satellites had observed several dozen gamma-ray events of an unknown nature localized in interstellar space far from Earth. A list of two dozen events was published by the leader of the Vela equipment team, Klebesadel [1], which started research on a new astrophysical phenomenon called cosmic gamma-ray bursts.

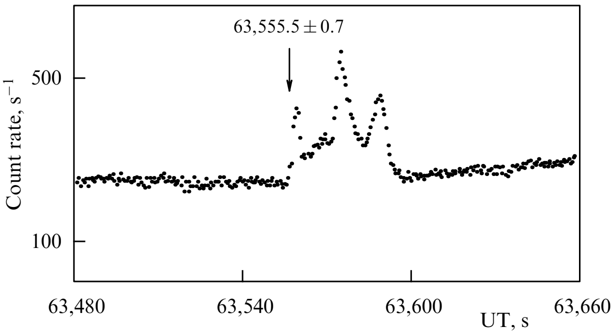

Figure 1. One of the first independent confirmations of the discovery of cosmic GRBs: GRB 720117 as observed by the Ioffe Institute experiment aboard the Kosmos-461 satellite.

From the middle of the 1960s, the Ioffe Physical-Technical Institute (PTI) carried out studies of cosmic radiation in the range 30 keV–4.1 MeV and its variability using Kosmos, small satellites in low-Earth orbits. This research was initiated by academician B P Konstantinov. A dedicated scintillation gamma-spectrometer was designed and manufactured that was equipped with a multichannel pulse-height analyzer coupled with an ultrasonic delay-line internal memory unit [2]. It was one of the world's first multichannel amplitude analyzers with internal memory ever used in a space experiment. It enabled measuring temporal variations of the gamma-ray flux and their energy spectra with a reasonable accuracy. The experiments aboard Kosmos-135, Kosmos-163, and Kosmos-461 satellites allowed accurately estimating the flux of gamma rays produced in Earth's atmosphere by primary cosmic rays using the dependence of the gamma-ray intensity on the geomagnetic cutoff rigidity, and also allowed imposing an upper bound on the diffuse cosmic gamma-ray flux in the energy range 30 keV–3.7 MeV. The spectrum of the diffuse cosmic gamma rays was measured in the range 30 keV–4.1 MeV and a spectral feature at ~ 1 MeV was detected for the first time [3, 4]. These results showed that the early data obtained by the American ERS-18 satellite were incorrect and forced the American researchers to reconsider their data on the diffuse gamma-ray emission collected in the course of the Apollo program.

The instrumentation aboard the Kosmos-461 satellite included a rate meter with a time resolution of a fraction of a second. It is this detector that enabled one of the first independent confirmations of the discovery of cosmic GRBs by the American Vela satellites. A GRB from the list of events detected by Vela satellites in remote orbits was registered by the rate meter aboard the Kosmos-461 low-Earth spacecraft (Fig. 1) [5]. Based on this finding, the Ioffe Institute gained the opportunity to design and perform its own experiments aimed at studying this new astrophysical phenomenon aboard the automatic interplanetary missions Venera 11–14 in 1978–1983. This research was headed by E P Masetz.

For experiments aboard the Venera interplanetary missions, original high-sensitivity and high-performance scientific KONUS instrument (Fig. 2) [6, 7] was designed. Each spacecraft was equipped with six scintillation detectors with a diameter of 80 mm and a thickness of 30 mm with anisotropic angular sensitivity enabling autonomous determination of the GRB sky location. The detectors were placed along the positive and negative axes of the spacecraft (Fig. 2a). Each detector was equipped with a system of detailed time and amplitude analysis of gamma-ray emission from GRBs (Fig. 2b). In addition, the Ioffe Institute requested that the spacecraft be separated by distances of several million kilometers, which enabled a high-precision localization of GRBs by the triangulation method and provided an additional independent determination of their coordinates. One of the most important observational properties of GRBs detected by the KONUS experiment aboard the Venera 11–14 stations is the bimodality of the GRB durations, suggesting their various physical origins (so-called 'short' and 'long' bursts; Fig. 3a) [8]. Another important result established for the first time by the Venera 11–14 experiments is the homogeneous distribution of GRBs in the sky (Fig. 3b) [8], suggesting their extragalactic origin. Yet another property of GRBs found by the KONUS experiments is the correlation between the intensity of GRB emission and its spectral hardness [9], dubbed the 'Golenetskii relation' in the scientific literature.

In the 1990s, these results were confirmed by the BATSE experiment (Burst And Transient Source Experiment) aboard the Compton Gamma Ray Observatory (CGRO). The BATSE experiment found that the typical spectrum of short gamma-ray bursts is harder than that of long GRBs [10]. In

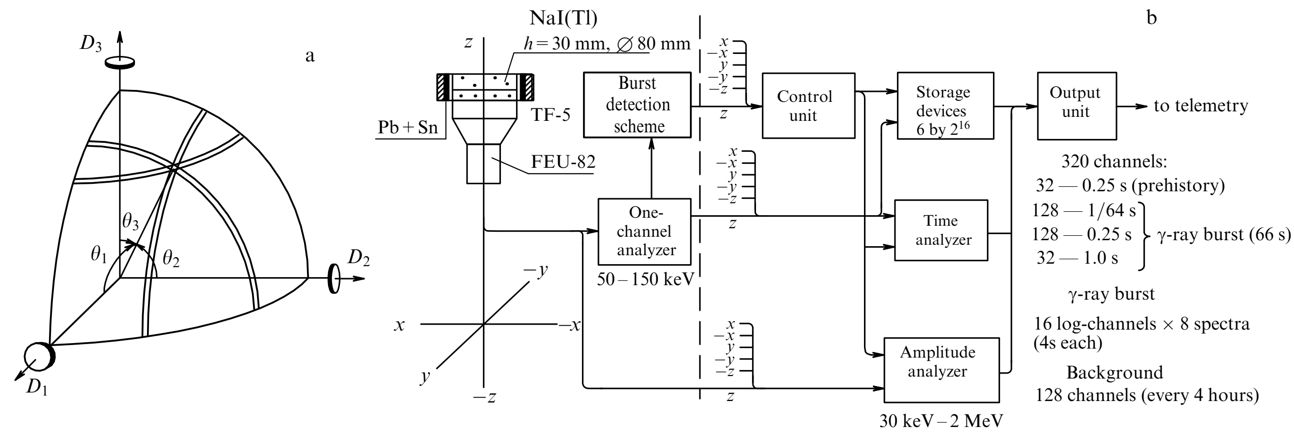

Figure 2. KONUS detector aboard Venera 11–14 spacecraft: (a) the scheme of allocation of detectors along axes of Venera 11–14 spacecraft; (b) the functional block diagram of KONUS detectors.

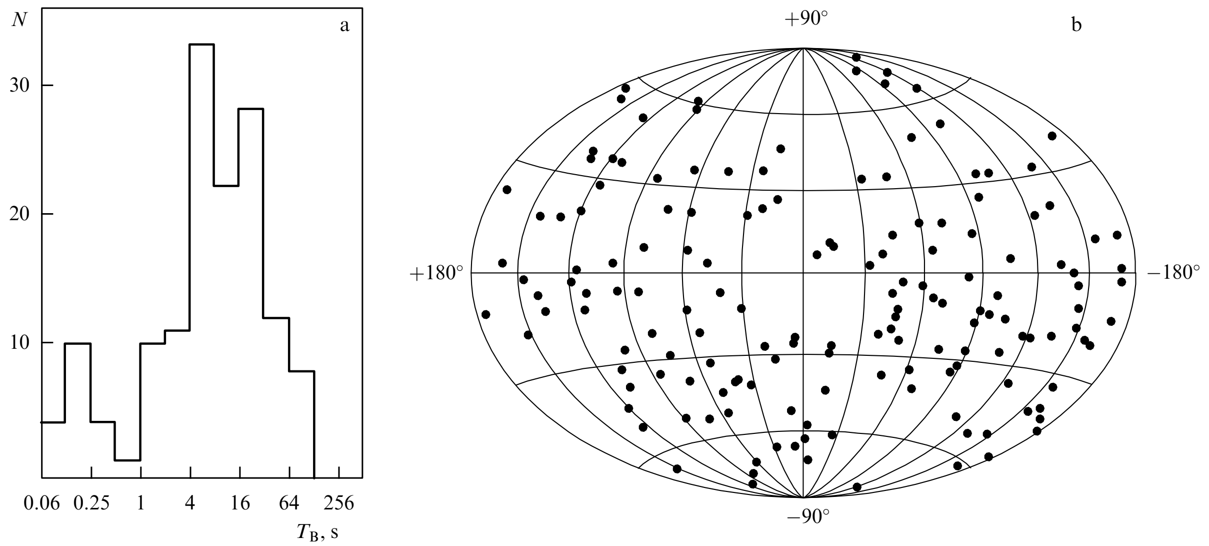

Figure 3. Key results of the KONUS experiment aboard Venera 11–14 spacecraft: (a) bimodal duration distribution of GRBs; (b) isotropic sky distribution of GRBs. T_B is the GRB duration, N is the number of events.

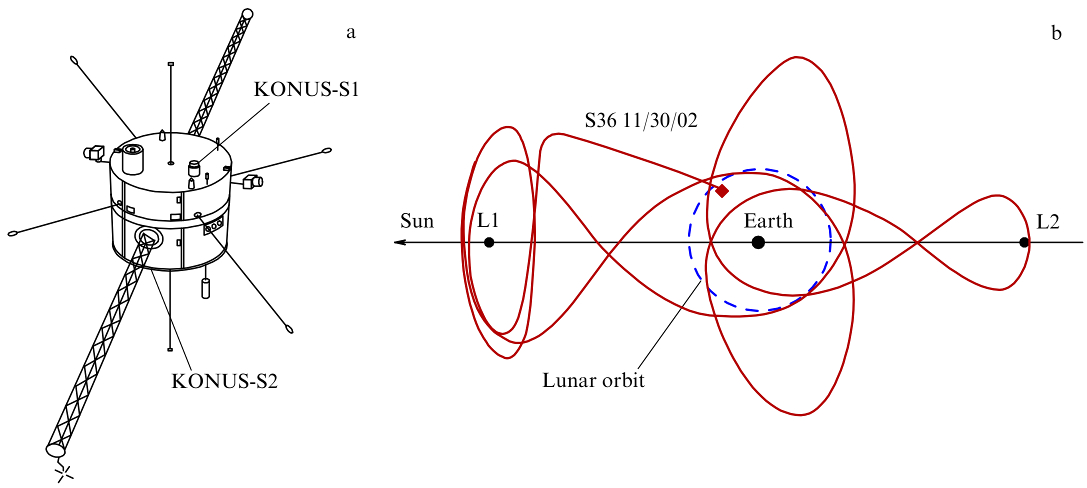

Figure 4. (a) GGS WIND satellite with KONUS detectors and (b) its orbit in interplanetary space.

addition, the wide spectral range ($\sim 20-2000$ keV) of BATSE revealed that the spectrum of a significant fraction of GRBs is essentially nonthermal and can be approximated well by a smoothly broken power-low function (the 'Band' GRB function) [11] with the break parameterized by the maximum energy in the νF_ν spectrum (E_p) with a typical value of E_p ranging from 100 to 1000 keV.

Since 1994, the KONUS experiments carried out by the Laboratory for Experimental Astrophysics of the Ioffe Institute have been continued in the international KONUS–WIND experiment [12] aboard the GGS Wind space observatory (NASA, USA). Over more than 25 years, the KONUS–WIND experiment has played an important role in GRB studies due to its unique characteristics (Fig. 4). The location of the satellite near the L1 Lagrangian point of the Sun–Earth system provides a stable radiation background and continuous sky survey by two NaI(Tl) detectors in a wide spectral range ($\sim$ 10 keV–10 MeV) with a high (up to 2 ms) time resolution. By the middle of 2018, KONUS–WIND has triggered $\sim$ 4600 times on various transient events, including $\sim$ 3000 GRBs, $\sim$ 260 SGR flares, and more than 1000 solar flares.

2. Soft gamma-ray repeaters

Soft gamma-ray repeaters (SGRs) are unique hard X-ray transients historically closely related to GRBs. The discovery of this class of transients is a fundamental result of the KONUS experiments aboard the Venera 11 and 12 missions, which detected an extremely bright GRB on March 5, 1979. Although the burst was registered by gamma-detectors from nine spacecraft [13–16], the most detailed light curve of this event was measured only by the KONUS detectors aboard Venera 11 and 12 interplanetary missions. The light curve consisted of an intense initial pulse transiting into a soft pulsating (with a period of $\sim$ 8 s) long 'tail' (Fig. 5) that was observed only by the KONUS detector due to its low energy threshold. The spectrum of the pulsating emission was well described by the optically thin thermal bremsstrahlung (OTTB) model with the temperature $kT \sim 30$ keV. We note that in the SIGNE II experiment, several pulses were detected [17]. The next day, on March 6 1979, two repeated bursts were detected from this source. The position of the sources determined by the triangulation method coincided with the N49 supernova remnant in the Large Magellanic

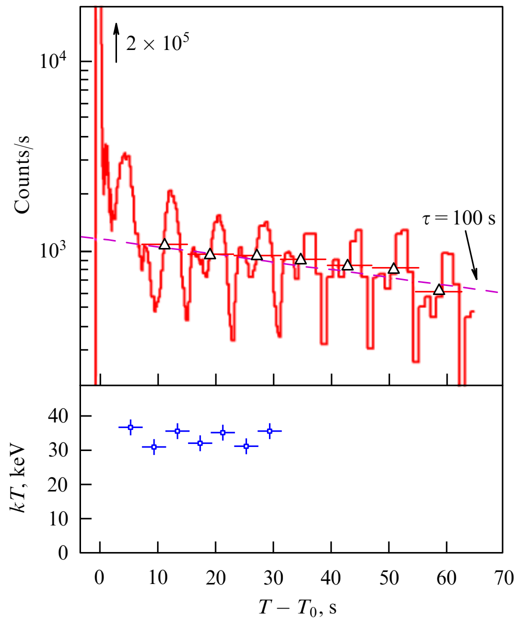

Figure 5. Discovery of SGRs by the KONUS experiment aboard Venera 11 and 12 missions. The March 5, 1979 event is the first observation of a giant outburst from SGR 0526–66.

Cloud at a distance of 55 kpc, which for the first time suggested a possible relation between SGR sources and neutron stars. This source was later called SGR 0526–66. In the same 1979, another gamma-ray repeater, SGR 1900 + 14, was discovered by the KONUS experiment [18].

At the end of the 1980s, the third then known soft gamma-ray repeater SGR 1806–20 was discovered in the Galactic bulge [19]. Most of the observed repeated bursts lasted less than one second and had a softer spectrum than that of nonrepeating GRBs. Based on these facts, the hypothesis was put forward in [20] that the known sources of repeated gamma-ray bursts had another origin than ordinary GRBs and were likely related to neutron stars.

Today, more than 20 SGRs are known, most of which are associated with slowly rotating (period $P \sim 2-12$ s) rapidly spinning-down ($\dot{P} \sim 10^{-13}-10^{-10}$ s s^{-1}) isolated neutron stars. The dipole magnetic field as inferred from the spin-down rate is estimated to be in the range $10^{13}-10^{15}$ G, which is several orders of magnitude stronger than in radio pulsars. The magnetar population includes both SGRs and anomalous X-ray pulsars (AXPs) with high X-ray luminosity [21, 22]. These objects show a high soft (< 10 keV) X-ray luminosity $\sim 10^{34}-10^{35}$ erg s^{-1}, exceeding the rotational energy loss rate by a neutron star derived from the magneto-dipole formula. For SGRs, the X-ray fluxes increase by several orders of magnitude during the active outburst stage [23]. Both steady soft X-ray emission and outburst hard X-ray radiation are thought to be due to the dissipation of the neutron star's magnetic energy (stored in currents supporting the magnetic field).

SGRs demonstrate two types of hard X-ray (10–1000 keV) activity. During the active stage, SGRs emit short (0.001–1 s) hard X-ray bursts with a peak luminosity of $10^{38}-10^{42}$ erg s^{-1}. The active phase duration can be from several days to years, followed by a prolonged quiescence stage. Much more rarely, possibly once during the entire SGR stage, giant outbursts can occur on magnetars with a huge energy release of $(0.01-1) \times 10^{46}$ erg [23]. To date, giant flares have been observed only in three sources: SGR 0526–66 in the Large Magellanic Cloud, and SGR 1900 + 14 and SGR 1806–20 in our Galaxy. All these flares were studied in detail by the KONUS experiments [13, 24, 25].

The unique data enabling a detailed estimate of the energy release in the initial peak of the giant flare of SGR 1806–20 on December 27, 2004 were obtained by the KONUS–WIND and HELICON experiments of the Ioffe Institute [25]. The radiation fluxes in the initial pulses of giant flares are so high that scintillation gamma-ray detectors aboard spacecraft saturate, making it impossible to carry out measurements. This was the case for the KONUS–WIND and other space gamma-ray detectors during the giant gamma-ray flare on December 27, 2004. However, the situation with observations of this event turned out to be nonstandard thanks to the simultaneous HELICON experiment aboard the KORONAS-F satellite in a low-Earth orbit. The HELICON detectors were similar to those of KONUS–WIND. Due to its near-Earth location, during the giant SGR flare, the HELICON detectors were screened by Earth. However, the initial peak was so bright that the HELICON detectors were able to register its reflected pulse from the surface of the Moon (Fig. 6). Analysis of the reflected emission enabled the correct reconstruction of the time profile of the giant flare (Fig. 7) and the estimation of its total energy, 2.3×10^{46} erg, and peak luminosity, 3.5×10^{47} erg s^{-1} (by assuming the source distance of 15 kpc), which turned out to be several orders of magnitude higher than the energy of previously observed giant flares (see Table 3 in [26]).

The detection of such a powerful giant flare revived the idea of possible observations of similar events in nearby galaxies, first proposed in [27, 28]. The initial pulse of the flare can be observed like an ordinary cosmological short GRBs. The results of searches for such events are presented in [29]. Such a search, using the largest KONUS–WIND short GRB sample, revealed that magnetars can generate a giant flare less often than approximately once per century and that the fraction of extragalactic giant flares among relatively bright short GRBs is less than 10% [30]. Only two extragalactic giant SGR flare candidates were detected over the operation time of the KONUS–WIND experiment. GRB 051103, detected by the Interplanetary Network (IPN), was associated with the galaxy group M81/M82 at a distance of 3.6 Mpc (see, e.g., [31]). The localization of the other bright short GRB 070201 [26] overlaps the spiral arm of the Andromeda galaxy; here, the source power is in agreement with other known giant flares. The giant SGR flare hypothesis is supported by a comparison of the spectral and energetic parameters of short KONUS–WIND GRBs and GRB 070201, showing that this flare is a clear statistical outlier [32].

The first fundamental ideas on the nature of SGR flares were proposed in [33, 34]. Based on the modulation period of the tail of the March 5, 1979 flare and the estimated age of the supernova remnant, a hypothesis was proposed that a *magnetar* — a young neutron star with a superstrong magnetic field of $\sim 10^{14}$ G — can be the source of the flare. The direct measurement of the neutron star spin-down in SGR 0526–66 and the corresponding age (1500 yrs) and magnetic field ($\sim 8 \times 10^{14}$ G) estimates were obtained in 1998 [35]. Such a magnetic field exceeds the quantum-electrodynamic limit $B_{\rm QED} = m_e^2 c^3/e\hbar \approx 4.4 \times 10^{13}$ G at

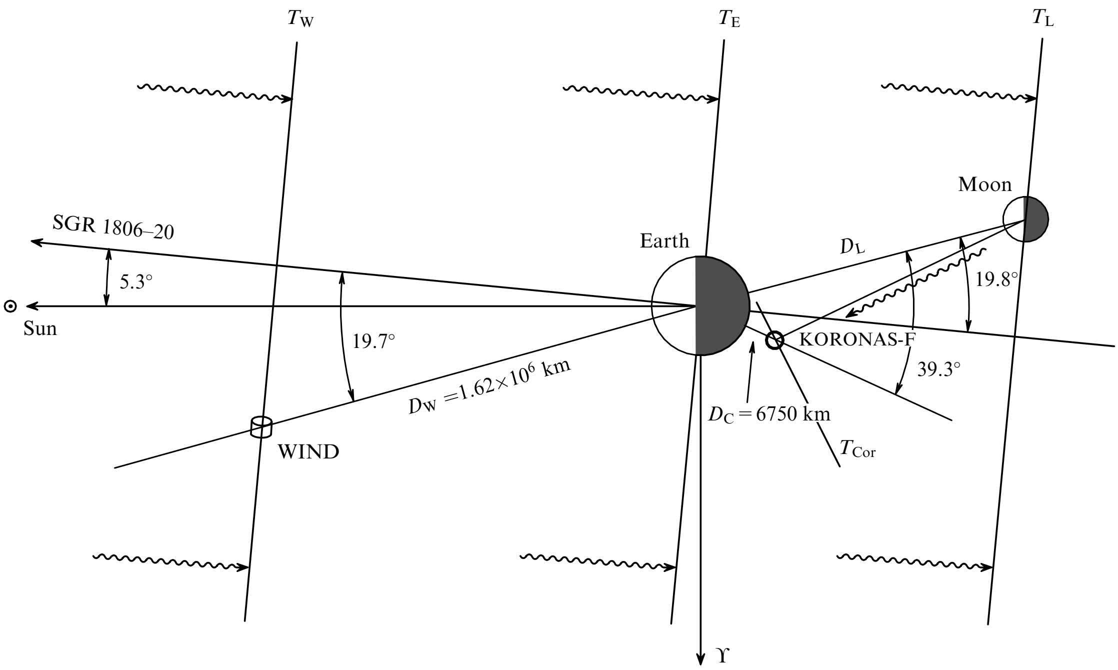

Figure 6. Diagram of observations of the giant outburst from SGR 1806–20 on December 27, 2004. Reflected from the Moon and strongly attenuated, the initial pulse from the event was detected by the HELICON detector aboard the KORONAS-F satellite.

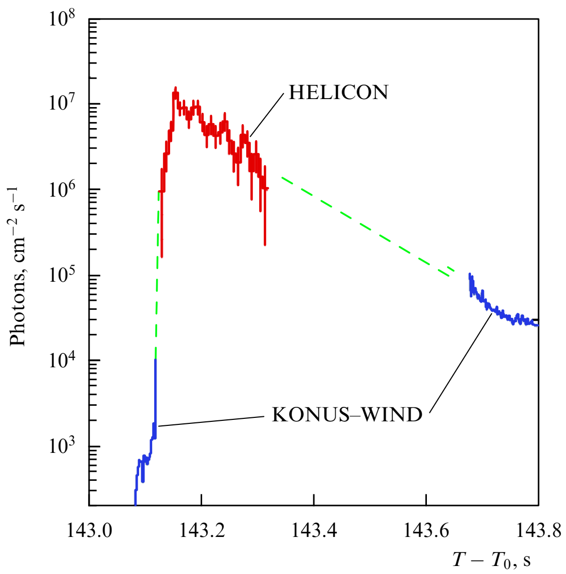

Figure 7. (Color online.) Time profile of the initial pulse of the giant outburst from SGR 1806–20 as recovered from KONUS–WIND and HELICON experiments.

which the energy of the first Landau level is comparable to the electron rest-mass energy. Quantum effects are important in describing processes in such magnetic fields. The magnetic field energy density is $W_B \approx 4 \times 10^{28} B_{15}^2$ erg cm^{-3} (where B_{15} is the magnetic field in units of 10^{15} G). To provide the observed energy of giant flares, the magnetic field should dissipate in a volume 10 km in diameter, of the order of the neutron star size. According to SGR models [22, 34], the rapid energy dissipation by the magnetic field reconnection heats the electron–positron plasma to relativistic temperatures. For the observed flare radiation to go out of the SGR source, a relativistic plasma outflow should be formed at distances of several thousand neutron star radii, enabling the circumvention of the problem of the initial Compton opacity of hot $e^{\pm}$-plasma. A detailed modeling of the formation of superstrong magnetic fields and their dissipation, as well as of nonstationary processes in magnetar magnetospheres, holds a number of unsolved problems and has been actively discussed in the literature (see, e.g., [22] for a review).

3. Modern multi-wavelength studies of gamma-ray bursts

3.1 Multi-wavelength observations and cosmological era of gamma-ray burst studies

Until the late 1990s, the origin of GRBs was unclear. The combination of the sky anisotropy of GRB sources and the shape of their cumulative flux distribution (the $\log N - \log S$ relation) [36] suggested their extragalactic origin. However, their localization error boxes in the sky obtained by noncollimated detectors, even using the triangulation method with spacecraft separated by millions of kilometers, were a fraction of a square degree at best.[1] The GRB error boxes contained thousands of astrophysical objects, preventing the identification of GRB sources.

In 1996, the Italian–Dutch space observatory BeppoSAX was launched. It was equipped with a GRB monitor and synchronously operating X-ray telescope WFC with a wide

[1] When a GRB is detected by two spacecraft separated by a distance d, its location is known to be within an annulus on the sky. The crossing of several annuli (when being detected by three or more satellites) yields the so-called 'error box'. The width of the annulus is determined by several factors: the length of the triangulation base d, the signal-to-noise ratio (SNR) in the correlated GRB light curves, and the time resolution δT. The combination of a long base with high SNR and small δT in practice is rarely achievable due to weight, size, and telemetry restrictions of interplanetary missions.

field of view (up to several minutes), providing high-precision real-time sky localization of X-ray sources associated with GRBs. This mission started the multiwavelength identification of GRB sources.

The detection of the X-ray afterglow of GRB 970228 [37], its subsequent identification with a transient optical source [38], and detection of the host galaxy at the redshift $z = 0.695$ [39] reliably confirmed the cosmological nature of GRBs [40–43]. The first estimate of the distance to a GRB obtained solely from spectroscopic observations of its afterglow appeared several months later, for GRB 970508. The redshift of the source was $z = 0.835$ [44], corresponding to a of ~ 7 billion years and the age of the Universe 6.5 billion years after the Big Bang.

Subsequent simultaneous observations of GRBs in hard and soft X-ray bands were carried out by the HETE-2 (High-Energy Transient Explorer) space observatory operating in the 2–400 keV range. HETE-2 discovered a new class of transients (XRFs, X-Ray Flashes) similar to GRBs but showing a much softer spectrum with $E_{\rm p} \sim 1-10$ keV.

In the those experiments, the typical time delay between GRB detection and optical follow-on observations performed to localize its sky position was about several hours. The situation changed dramatically in 2004 with the launch of the Swift space observatory [45] (the Neil Gehrels Swift observatory since 2017). The fast (about one minute) and accurate (of the order of a few angular seconds) localization of GRBs by Swift made it possible to obtain nearly real-time identification of events and to study the transition of the proper GRB radiation to multi-wavelength afterglow emission. The high sensitivity (up to 10^{-8} erg cm^{-1}) of the Swift–BAT (Burst Alert Telescope) system to relatively soft 15–150 keV gamma-ray emission enables effective registration of GRBs at high redshifts (up to $z \approx 9$) and weak short GRBs and SGRs. We note that the peak energy of a significant proportion of GRBs falls outside the Swift–BAT spectral range and cannot be directly estimated from the Swift–BAT observations.

The Swift data shed new light on the nature of short GRBs. In 2005, Swift detected an X-ray afterglow from the short GRB 050509B [46]. The X-ray afterglow from this GRB was weak and decreased below the detection threshold within a few hours. No optical afterglow was detected (the Swift–UVOT upper limit of the V-flux at 550 nm was 19.7 mag for the time delay of less than 300 min after the Swift–BAT GRB trigger). In the Swift–XRT (X-Ray Telescope) ~ 10 arcsec error box, an elliptical galaxy with a low star formation rate was identified at the cosmological redshift $z = 0.225$.

Shortly after that, two other short GRBs GRB 050709 (HETE-2) and GRB 050724 (Swift) were detected. For GRB 050709, the optical afterglow was detected for the first time, enabling its localization with an accuracy of better than one arc second. The GRB source was found on the outskirts of a galaxy with active star formation at the redshift $z = 0.160$. For the short GRB 050724, the X-ray to radio afterglow was detected for the first time. The host galaxy redshift was found to be $z = 0.257$. The intensity of the X-ray and optical afterglows of short GRBs turned out to be an order of magnitude lower than that of long GRBs, which provided an explanation for the lack of afterglow detection in previous events.

In June 2008, the GLAST space observatory (later named after Enrico Fermi: Fermi Gamma-Ray Space Telescope) was launched. The observatory is equipped with a gamma-ray burst monitor (GBM, 8–40 MeV) [47] and a large-area telescope (LAT, 20 MeV–300 GeV) [48], which make it possible to study GRBs in a broad energy range. The GRB energy spectrum was found to span up to several tens of GeV (see, e.g., [49]). A delay and longer duration of high-energy GRB emission relative to softer GRB emission were found, suggesting different generation mechanisms.

In the era of cosmic GRB research by specialized gamma- and X-ray telescopes, GRB observations by all-sky detectors not restricted by low-orbital conditions are important. By the middle of 2018, KONUS–WIND had triggered on ~ 3000 GRBs (the detection rate is ~ 120 events per year). These results are presented, in particular, in the short GRB catalogue [32] (about 300 events detected in 1994–2010) and in the catalogue of GRBs with known redshift [50] including 150 sources, of which 12 events are related to type I (short/hard) and 138 to type II (long/soft). These GRBs represent the most complete sample in the proper cosmological frame obtained from a systematic analysis of uniform broadband observations.

The KONUS–WIND experiment is a key vertex of the Interplanetary Network (IPN) of gamma-ray detectors [51, 52], consisting of 7 satellites, including the Mars–Odyssey space mission at a distance of up to 360 mln km (~ 1200 light seconds) from Earth. The IPN has a flux sensitivity of $\sim 6 \times 10^{-7}$ erg cm^{-2} s^{-1} and is able to localize up to 300 GRBs a year by the triangulation method. About 60% of these bursts are not observed by detectors with high angular resolution, and in many cases the IPN localization allows reducing the Fermi GBM/LAT error boxes. The IPN plays an important role in multiwavelength GRB observations, in particular, in combination with ground-based transients monitoring facilities like MASTER [53] and iPTF/ZTF [54, 55]. The IPN data are also used to search for gamma-ray emission from sources of gravitational waves, high-energy neutrinos, and giant outbursts from soft gamma-ray repeaters in nearby galaxies.

3.2 Classification of gamma-ray bursts

The duration distribution of GRBs demonstrates two pronounced peaks with maxima at ~ 0.3 s and ~ 30 s [10]; the boundary between the peaks at ~ 2 s conventionally separates short and long GRBs. This classification, complemented with information about the spectral hardness of GRB emission, made it possible to single out two clusters of events on the hardness–duration plane: short/hard and long/soft GRBs (Fig. 8).

This clusterization, suggesting the existence of two physically different types of sources, was discovered long before the distances to GRBs were measured. We emphasize that the observed duration and spectral hardness of GRBs do not completely reflect the proper source characteristics due to cosmological time dilation and spectral softening. However, with growing information on GRB redshifts, it became clear that the existence of two GRB clusters on the hardness–duration diagram is confirmed in the cosmological rest frame (at least at redshifts $z < 2$, common for short/hard and long/soft GRBs [50]).

Long/soft GRBs have been related to core collapses of young massive stars (type II), as suggested by observations of their host galaxies and association with accompanying supernovae (see Section 3.4). At the same time, short/hard GRBs most likely occur during the coalescence of compact objects (type I): of two neutron stars or a neutron star and a black hole (see Section 3.6).

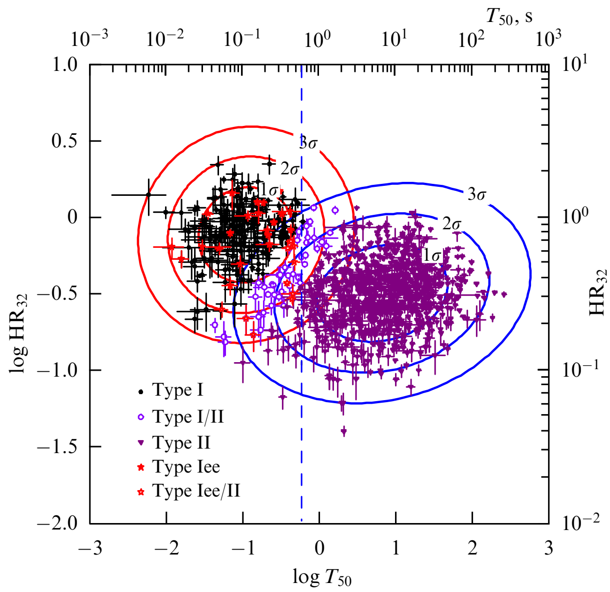

Figure 8. (Color online.) Classification of GRBs detected by KONUS–WIND. Clusters on the spectral hardness–duration plane reflect two physically distinct events: type I — short/hard bursts (compact binary coalescences) and type II — long/soft (massive star core collapses) [32]. HR_{32} is the integral 200–750 keV to 50–200 keV count ratio, T_{50} is the integration time of 50% of 50–750 keV counts from a GRB.

Of special interest are so-called 'ultra-long' GRBs lasting from a thousand to several thousand seconds [56]. The importance of studies of ultra-long GRBs are important, in particular, because their observed characteristics are close to those of the tidal disruption of stars by massive black holes. To date, about a dozen ultra-long GRBs have been studied in detail by different groups [57]. A significant advantage of the KONUS–WIND experiment due to its interplanetary space location is the possibility of observing ultra-long GRBs over their total duration, attaining several hours (Fig. 9) [58].

3.3 Gamma-ray burst energetics

The GRB redshifts are typically measured from optical spectral features (emission and absorption lines) in the host galaxy and/or afterglow or photometrically. Up to the present time, redshifts have been determined for about 500 GRBs ranging from $z = 0.0087$ (GRB 980425) to $z = 9.4$ (GRB 090429B). The detection of the brightest GRBs like the ultraluminous GRB 110918A [59] is possible up to $z \approx 17$ [50], i.e., to the epoch of hundreds of million years after the Big Bang.

The huge power of the explosion is one of the key parameters that are important for understanding the physics of GRB progenitors, their central engine, and the emission mechanism. The redshift of a GRB enables estimating its isotropic-equivalent energy ($E_{\rm iso}$), the energy release from its central engine, and the peak luminosity ($L_{\rm iso}$) characterizing the conversion of the kinetic energy of the explosion into radiation. With the high GRB energy fluxes (up to 10^{-3} erg cm^{-2} s^{-1}) and cosmological distances, these GRB characteristics attain enormous values: $E_{\rm iso} \sim 10^{55}$ erg (GRB 080916C) [60] and $L_{\rm iso} \sim 5 \times 10^{54}$ erg s^{-1} (GRB 110918A) [59], comparable to the rest-mass energy of the Sun and the steady luminosity of all stars in the visible Universe. The cumulative $E_{\rm iso}$ distribution of GRBs obtained from the latest KONUS–WIND and Fermi–GBM measurements [50, 61] exhibits an exponential cutoff at $E_{\rm iso} \sim 10^{54}$ erg (Fig. 10, upper plot), suggesting the observed limit of GRB energy release. At the same time, the GRB peak luminosity distribution (the luminosity function) [50] with a break at $L_{\rm iso} \sim 10^{53}$ erg s^{-1} keeps the power-law shape up to the uppermost boundary found so far (Fig. 10, bottom plot).

The huge energy release of GRBs was first explained for GRB 990510 [62] by assuming a strong jet beaming. For typical jet collimation angles of several degrees, the energy release for most GRBs is $\sim 10^{51}$ erg, which is comparable to supernova energies. Such an extreme energy release compar-

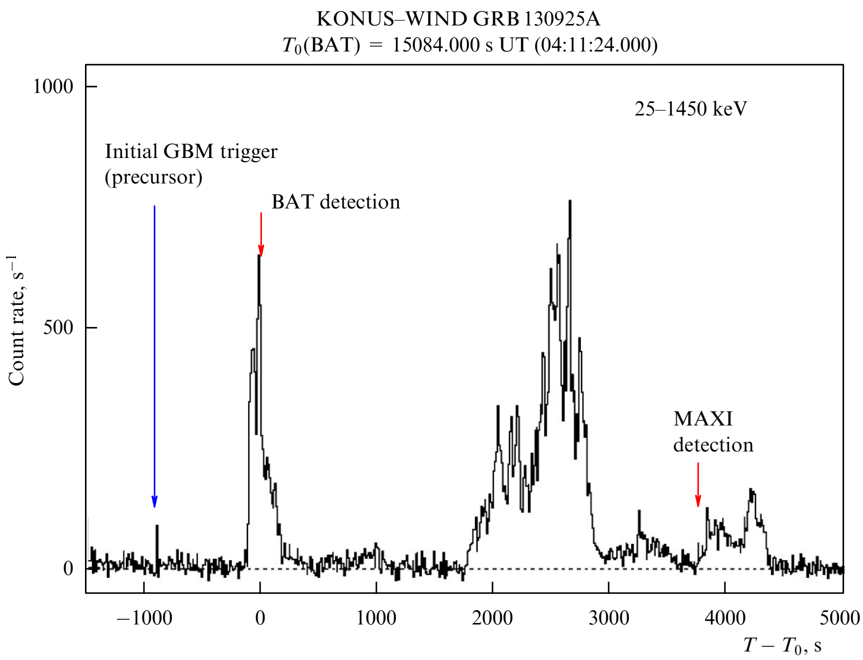

Figure 9. KONUS–WIND observations of the ultra-long GRB 130925A. The arrows show the moments of detection of separate parts of the event by other experiments. Shown is the light curve lasting about 6000 s.

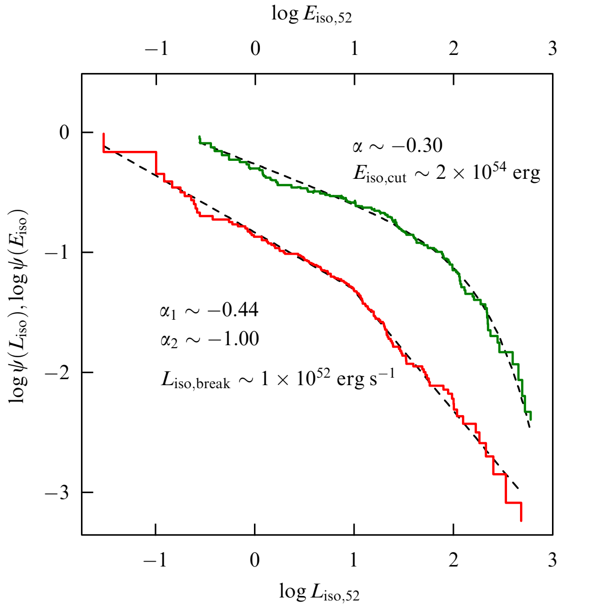

Figure 10. (Color online.) Cumulative peak luminosity $\psi(L_{iso})$ (bottom plot) and total energy $\psi(E_{iso})$ (upper plot) distributions of 'long' GRBs detected by KONUS–WIND [50]. Best-fit broken power-law ($\psi(L_{iso})$) and power-law with exponential cutoff ($\psi(E_{iso})$) approximations are shown.

able to the binding energy of a star on a time scale of the order of a few seconds suggests the relation of GRBs to core collapses of massive stars or coalescences of compact relativistic objects.

3.4 Long gamma-ray bursts and supernovae

The first observational evidence of the GRB–supernova connection was obtained in 1998 when type-Ic SN 1998bw was discovered within the error box of GRB 980425 ($z = 0.0085$, 35.6 Mpc) [63]. The peak of the optical light curve was observed at 10–20 days after the GRB. The discovered supernova was unusual. Modeling showed that it was 10 times as powerful as an ordinary supernova (10^{51} erg) and had a relativistic expansion velocity of ~ 0.1 times the speed of light. Due to these unique properties, SN 1998bw was called a 'hypernova' [64]. The isotropic equivalent of the peak luminosity of GRB 980425 was about $L_{iso} \sim 5 \times 10^{46}$ erg s^{-1}, a few orders of magnitude below that of most GRBs detected so far ($\sim 10^{50} - 10^{54}$ erg s^{-1}); such GRBs are usually the so-called low-luminosity GRBs. Only five years later, HETE-2 was able to detect the supernova SN 2003dh on top of the decaying afterglow from nearby GRB 030329 with the characteristic luminosity $L_{iso} \sim 8 \times 10^{50}$ erg s^{-1}.

To date, about 50 supernovae associated with relatively close GRBs at $z = 0.0085 - 1.0$ have been discovered [65]. We note that redshifts of long GRBs span a wide range $0.0085 - 9.4$ with the mean value $z \approx 2.3$.

For both ordinary type-Ibc supernovae and GRB-related supernovae, it is possible to estimate the shock velocity from radio observations (see, e.g., [66]). In the case of GRB-related supernovae, the radio emission is thought to be associated with the relativistic jet. The parameters of a slower component responsible for the observed supernova emission are derived from the modeling of the optical light curves and spectra. In the coordinates (shock velocity, ejecta kinetic energy), relativistic supernovae without a GRB (SN 2009bb and SN 2012ap), low-luminosity GRBs, and ordinary GRBs form a sequence as the velocity and kinetic energy of the ejecta increase. Such a sequence may suggest different jet formation scenarios: in the least energetic relativistic supernovae, the jet does not break out the stellar surface; in low-luminosity GRBs, the jet loses most of its energy to propagate through the stellar envelope (shock break-out GRBs); and in ordinary GRBs, the jet successfully escapes into the interstellar medium by losing an insignificant proportion of its energy (see, e.g., [65, 67]).

The brightest GRB supernova detected so far is SN 2011kl, associated with the ultra-long GRB 111209A. Its brightness cannot be explained by radioactive ^{56}Ni decay only. It is assumed that its emission is maintained by the central GRB source, for example, by a magnetar [68]. Further detection of supernovae associated with GRBs should give new information on the physics of GRBs and their progenitors.

3.5 Gamma-ray bursts, cosmology, and fundamental physics

After the discovery of the X-ray and optical afterglows of the long GRB 970228 [37, 38], the measurement of the cosmological redshift of GRB 970508 [44] and the discovery of the first SN 1998bw associated with the long GRB 980425 [63], sources of long GRBs were reliably related to the final evolutionary stages of massive stars in galaxies at cosmological distances (see, e.g., [69]). A subsequent detailed modeling of a rotating iron core collapse into a black hole (the 'collapsar' model [70]) showed that under some initial conditions, a relativistic jet with an opening angle of $\sim 10°$ and a kinetic energy of $\sim 10^{52}$ erg can form, which can explain the observed characteristics of most long GRBs in galaxies with active star formation.

Due to their huge luminosity, GRBs are unique tools to probe the Universe over all of its history. In particular, GRB population studies provided constraints on the Universe expansion parameters and dark energy properties in a broad range of redshifts. This problem is tightly related to the possibility of using GRBs as 'standard candles' [2] for independent luminosity distance measurements. Unlike type-Ia supernovae, whose luminosity is closely related to the fundamental Chandrasekhar mass limit for white dwarfs, the main difficulty with GRBs is the observed broad range of their power and luminosities. The GRB 'standardization' could be performed using phenomenological correlations [72, 73] between the GRB energetics and spectral hardness (the so-called 'Amati' [74] and 'Yonetoku' [75] relations and their 'collimated' versions [76]). The most complete data on GRB energy and hardness correlations were obtained from the analysis of 150 GRBs with known redshifts detected in the KONUS–WIND experiment [50]. In particular, it was shown in [50] that the sharp 'lower' boundary of the 'Amati' and 'Yonetoku' relations (for relatively soft bright events) is determined by the properties of the GRB population, whereas the 'upper' bound for relatively hard faint GRBs is largely caused by observational selection effects. Thus, the use of GRBs as 'standard candles' remains an open issue.

The association of long GRBs with core collapses of massive stars [77] is the key feature enabling the estimation

[2] The idea of using GRBs as 'standard candles' was first suggested by Lipunov, Postnov, and Prokhorov in 2001 [71].

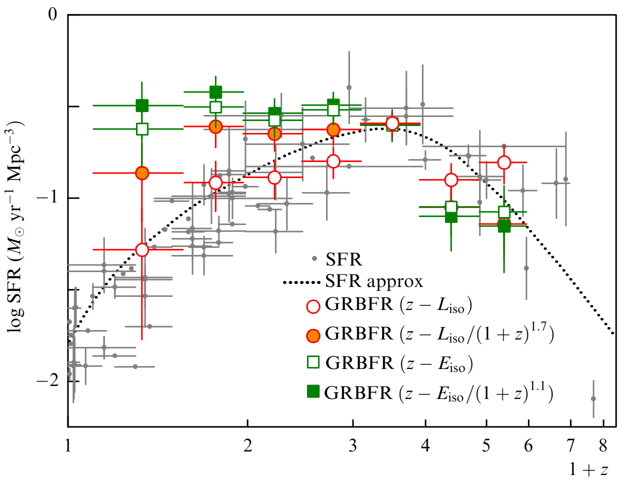

Figure 11. (Color online.) Relative GRB formation rate (GRBFR) as a function of the redshift z from the KONUS–WIND experiment [50]. The results corrected due to theosmological evolution of luminosity and energy (colored symbols) suggest a GRBFR excess over the cosmological star-formation rate (SFR) at low z. Grey symbols show SFRs from [78–81]. The dashed line shows the SFR approximation from [82].

of the star formation rate in galaxies in a broad range of redshifts. The gradual increase in statistics of GRBs with known redshifts enables the determination of the global GRB population characteristics, including the luminosity function and cosmological evolution of the GRB formation rate (GRBFR). Figure 11 shows the GRBFR obtained for KONUS–WIND long bursts in the range of redshifts z from 0.125 to 5, which demonstrates an excess relative to the cosmological star formation rate (SFR) at low redshifts ($z < 1$) [50]. This result may suggest either the diversity of the physical nature of long GRBs or the cosmological evolution of their progenitors. On the other hand, the estimated GRBFR is in good agreement with the SFR history at high z, suggesting that observations of remote GRBs can be used to estimate SFR and the initial stellar mass function in the early Universe. In particular, GRBs at the reionization stage ($z > 6$) can be produced by the first population-III stars with masses exceeding 100 solar masses. Theoretical modeling of their collapses in [83, 84] shows that the total energy release in such GRBs should be $> 10^{54}$ erg with a relatively low luminosity $\sim 10^{52}$ erg s^{-1}. Thus, the discovery of distant GRBs with a high total-energy-to-luminosity ratio could be direct observational evidence of the first stars in the Universe.

GRB afterglows with a nonthermal continuum initial spectrum passing through the interstellar medium of the host galaxy and the intergalactic medium acquire absorption features carrying information on the elemental abundance and ionization degree of matter on the line of sight. When detecting several dozen GRBs at $z \sim 7-9$, it could help to assess the history of the metallicity, conditions, and main sources of hard radiation in the reionization epoch (see, e.g., [85]). The detection of CO absorption bands in the GRB afterglow spectra could help to estimate the CMB temperature evolution and possible variation of physical constants at redshifts $z > 3$, inaccessible previously [86].

The Fermi–LAT detection of high-energy photons from GRB 090510 [87] with a high time resolution made it possible to impose constraints on quantum gravity models with Lorentz invariance violation, which predict the dependence of the photon propagation velocity v_{ph} on its energy E_{ph}. In some models (see, e.g., [88]), the dependence

$$v_{ph} = \frac{\partial E_{ph}}{\partial p_{ph}} \approx c\left[1 - \frac{n+1}{2}\,\zeta_n\left(\frac{E_{ph}}{M_{QG}c^2}\right)^n\right]$$

is considered, where n defines the linear ($n = 1$) or quadratic ($n = 2$) character of the lowest term in the decomposition of the modified dispersion relation for photons, $\zeta_n = \pm 1$, and M_{QG} is the characteristic mass scale of quantum gravity. In GRB 090510, a photon with an energy of about 31 GeV was registered in a time of less than one second after photons with an energy of a few MeV, which allowed establishing the bound $M_{QG} > M_P$ for $n = 1$, where the Planck mass is $M_P = 1.22 \times 10^{19}$ GeV [89].

In addition, multiwavelength GRB studies can be used to probe the Einstein equivalence principle, which, in particular, postulates that the time delay during the propagation of a photon in a gravitational field (Shapiro delay) should not depend on the photon energy. Important results in this field were obtained from multiwavelength observations of GRB 050820 [90] and GRB 080319B [91]. The optical emission from the first of these was detected by the RAPTOR telescope at the Los Alamos National Laboratory (USA). A comparison with the data recorded by KONUS–WIND provided the first observation of the simultaneous beginning of the optical and gamma emission from a GRB. The second GRB was the brightest optical GRB with a maximum visible optical luminosity of 5.3 mag and a gamma-ray fluence of $\sim 6 \times 10^{-4}$ erg cm^{-2} (Fig. 12). A joint analysis of the data collected by the KONUS–WIND gamma-ray detector and the ground-based Pi of the Sky optical monitor showed that the gamma-ray and optical emission from this burst starts and ends at the same time, reliably suggesting their origin within one spatial region. Based on this result, it was concluded in [92] that the post-Newtonian parameter γ is the same for optical and MeV quanta at the level of $(\gamma_{eV} - \gamma_{MeV}) \leqslant 1.2 \times 10^{-7}$, which is an order of magnitude better than constraints derived from the supernova SN 1987A observations.

3.6 Short gamma-ray bursts and gravitational waves

The assumption that GRB sources could be related to compact binary coalescences (a double neutron star or a

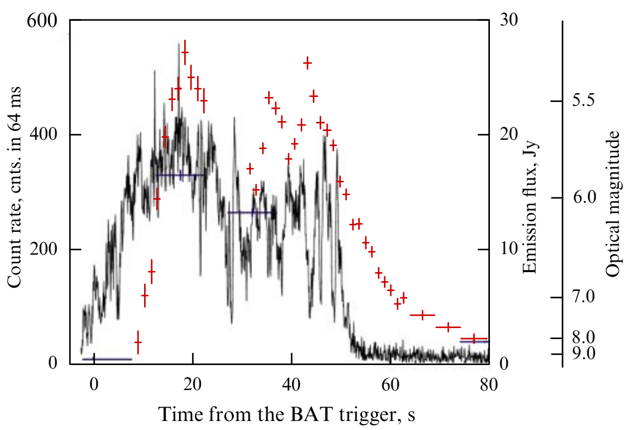

Figure 12. Simultaneous detection of gamma-ray emission (KONUS–WIND) and ultrabright optical emission (Pi of the Sky telescope) from GRB 080319B.

neutron-star–black-hole binary) had been put forward long before direct distance measurements to GRBs. Partially motivated by the fact that the characteristic merging time of the components of the Hulse–Taylor binary pulsar [93] is about 0.1 bln years, the first papers [94–96] pointed out that double neutron star coalescences could produce more than 10^{50} ergs in gamma rays, which could be typical for a cosmological GRB. Such coalescences in the absence of a dense surrounding interstellar medium could generate jets with a low baryon load that can be accelerated to relativistic velocities. A more detailed study of binary neutron star coalescence was performed in [97], noting that a short GRB progenitor can have a significant offset from the host galaxy center due to the velocity acquired by the binary system during neutron star formation. It was stressed that the coalescence must be accompanied by gravitational wave radiation within the frequency band of the ground-based LIGO interferometer [98]. It was also suggested in [96, 99] that binary neutron star coalescences can be potential sites of r-process nucleosynthesis.

By the middle of 2018, several dozen short GRBs had been associated with galaxies at redshifts $z \sim 0.1-1.3$; on average, they are more massive and contain an older stellar population than the host galaxies of long GRBs. The short GRB sources are located, on average, four times farther away from the host galaxy centers than long GRBs, which are mainly concentrated around the brightest ultraviolet regions in their host galaxies. No short GRBs were found to be associated with a supernova. The observed short GRB locations in host galaxies are in good agreement with the model distribution of binary neutron stars (see [100] and the references therein). Thus, observations suggest that many short GRBs are related to the old galactic population and can result from compact binary mergers.

Properties of gamma-ray emission from short GRBs have been widely studied in various experiments, including CGRO–BATSE, Swift–BAT, Fermi–GBM/LAT, and KONUS–WIND. The most complete sample of short GRBs was observed by KONUS–WIND (currently, more than 400 events). Further analysis of this sample in [32] revealed, in particular, that some of the short GRBs cannot be described by one spectral model (power law with a break or an exponential high-energy cutoff), and an additional power-law spectral component mainly contributing at low (< 50 keV) and high ($\gtrsim 2$ MeV) energies is needed. Analyses of bursts with the assumed extended emission (long-lasting weak emission observed after the main short gamma-ray pulse) showed that in contrast to the results of early studies, their spectrum can be sufficiently hard with a peak energy of up to several MeV. The study of the KONUS–WIND short GRB population on the hardness — intensity diagram revealed that the bursts generally follow the dependences $E_{\rm p} \propto S^{1/2}$ and $E_{\rm p} \propto F^{1/2}$, where $E_{\rm p}$ is the peak energy of the time-integrated spectrum, S is the burst fluence, and F is the peak energy flux, which is apparently a manifestation of the 'Amati' and 'Yonetoku' relations for short GRBs.

The very bright GRB 070201 falls out of the general population trend, suggesting that it can be a giant magnetar flare in the Andromeda galaxy.

By 2017, the last undiscovered elements in the physical picture of the short GRB phenomenon were the detection of gravitational waves from the coalescence of binary neutron stars and registration of optical emission from radioactive decay of elements produced by the r-process during neutron star disruption. These two features were simultaneously observed on August 17, 2017, when two LIGO detectors registered the signal from a coalescing binary neutron star at a distance of 40 Mpc, and 1.7 s after that a short GRB was detected by the Fermi and INTEGRAL gamma-ray observatories [101]. The initially large localization region of the gravitational-wave event was decreased to 28 square degrees using the joint analysis of the LIGO data and data from the European Virgo gravitational-wave observatory, which did not detect the gravitational-wave signal, suggesting that the source fell within the minimum sensitivity of the detector beam. The obtained localization region was in agreement with the autonomously found Fermi–GBM error box of the short GRB.

An additional constraint on GRB localization was obtained from the propagation time delay between the Fermi and INTEGRAL space observatories [102], enabling a more reliable identification of the short GRB with the gravitational wave source by reducing the Fermi–GBM error box by a factor of three. This method of GRB localization can reduce the sky area in present and future searches for electromagnetic transients in the case of less precise LIGO/Virgo localizations.

The short GRB 170817A accompanying binary neutron star coalescence had atypical parameters for the population of cosmological short GRBs. The event duration was ~ 2 s, and the light curve demonstrated two peaks: the initial pulse lasting ~ 0.6 s with a nonthermal spectrum with a maximum $EF(E)$ at around 200 keV, followed by subsequent thermal emission with a temperature of ~ 10 keV. At the distance of 40 Mpc, the isotropic energy of the burst was $\sim 5 \times 10^{46}$ erg, which is 2–6 orders of magnitude smaller than the typical value for short GRBs. This discrepancy can be explained, for example, in the model of a relativistic jet with a large viewing angle (see, e.g., [103]). This model is also indirectly supported by the late detection of X-ray and radio afterglows from this burst [104–106].

In the course of the day after the gravitational wave burst trigger, within its error box, an optical source of ~ 17 visual magnitude was discovered on the outskirts of a lenticular galaxy with a low star formation rate, located at a distance of 39.5 Mpc [107]. The first two optical spectra of the source measured during the first two days (0.6 and 1.5 days after the burst) were close to thermal with temperatures of 8300 K and 5500 K, and respective radii $R \sim 4.5 \times 10^{14}$ cm and $R \sim 7 \times 10^{14}$ cm, suggesting a source expansion velocity of $\sim 0.3c$. The blue light curve of the source rapidly decayed at a rate of ~ 2 stellar magnitudes per day. The red light curve exhibited a more complicated evolution: the decay at a rate of ~ 0.3 mag per day in the first one and a half days was followed by a plateau on the fourth day, with renewed decay after the ~ 8th day [108, 109]. The observed behavior of the optical transient can be described by a two-component jet produced by the coalescence of two neutron stars. In this model, the main contribution to the blue spectrum is due to lighter ($\sim 0.01 M_{\odot}$) and rapidly expanding (~ 0.3) ejecta along the binary system axis. The long-wavelength part of the spectrum is due to heavier ($\sim 0.04 M_{\odot}$) and more slowly expanding (~ 0.1) ejecta in the equatorial plane. The light curves and spectra strongly depend on the abundance of heavy elements produced in the r-process during the coalescence [110].

Thus, on the one hand, the nature of short GRBs seems to be well understood. A substantial part of them occurs in galaxies at cosmological distances, and their sources are closely related to merging compact binaries. On the other hand, there is a significant difference between the only short GRB 170817A known so far, related to binary neutron star coalescence, and the short GRB population. Furthermore, the generation mechanism of short bursts with extended emission, when the initial short pulse is followed by an extended (up to several hundred seconds) weaker emission, remains unclear [111–113].

The current LIGO/Virgo observation run started in April 2019 can increase the population of local (150–200 Mpc) optical and gamma-ray transients related to merging compact binaries, including binary neutron star mergers, which should provide deeper insight into processes during the tidal disruption of neutron stars.

4. Modeling of astrophysical processes with extreme electromagnetic energy fluxes

Extreme energy release comparable to the binding energy of a star over the characteristic time of the order of several seconds suggests a relation between GRBs and core collapses of massive stars or binary neutron star coalescences. The lack of conversion of gamma photons into electron–positron pairs in a compact emission source suggests a relativistic motion with Lorentz factors Γ comparable to or greater than 100. Indeed, without relativistic motion, a gamma-ray source with the characteristic variability time δt_0 must have the size less than $c\delta t_0$. The typical isotropic luminosity L_γ of GRBs at cosmological distances exceeds 10^{52} erg s^{-1}. The collision of two photons with energies ϵ_1 and ϵ_2 satisfying the threshold condition $(\epsilon_1\epsilon_2)^{1/2} > m_e c^2$ is accompanied by the creation of electron–positron pairs $\gamma\gamma \to e^+e^-$ with a cross section of the order of the Thomson cross section σ_T. For photons with energies ϵ above the reaction threshold, the optical depth of the system is

$$\tau_{\gamma\gamma} \sim \frac{\sigma_T L_\gamma}{4\pi c^2 \delta t_0 \epsilon} \,,$$

yielding $\tau_{\gamma\gamma} \sim 10^{12}$ for $\delta t_0 \approx 0.1$ s and $\epsilon \approx 1$ MeV. Such a huge optical depth should give rise to almost equilibrium thermal spectra, whereas GRBs demonstrate significantly nonthermal (broken power-law) gamma-ray spectra. The 'compactness problem' of GRBs can naturally be solved if there is a relativistic motion in the sources [95, 114–116].

The Fermi gamma-ray observatory reliably detected GeV gamma-ray photons during the main emission phase of GRBs. In the short GRB 090510 at the redshift $z = 0.903$ detected by the Swift, KONUS–WIND, INTEGRAL, AGILE, and other observatories, the Fermi–LAT telescope detected photons with energies up to 31 GeV. The 31 GeV photon arrived about 0.8 s after the GRB trigger. The presence of high-energy photons in the main phase of the burst enabled estimating the minimal Lorentz factor of the outflow as $\Gamma \sim 1200$. Moreover, in GRB 090510, a new hard gamma-ray component was discovered on top of the standard Band spectrum. This component cannot be easily explained using the one-zone model with synchrotron and synchrotron–Compton formation mechanisms of the main spectrum of the burst [89].

The observed gamma-ray spectra are significantly nonthermal, suggesting the conversion of most of the energy from the central engine into nonthermal particles with subsequent effective radiation from the accelerated particles, most likely by the synchrotron mechanism. This made it possible to model GRBs as dissipative relativistic outflows [117]. The relativistic outflows are most likely launched by binary neutron star mergers [96] or by massive star core collapses [118].

The construction of a detailed model of GRBs from first principles requires systematically taking many factors into account, including neutrino transport and turbulence in the 3D geometry (with GR effects), as well as a huge computer power, which is still unavailable. However, the existing models, based on the restricted description of the sources but taking the interaction of the relativistic outflows with the surrounding matter into account, can be used to interpret observations and restrict model parameters.

Collimated relativistic outflows (jets) can be formed during the collapse of rotating massive stars into a black hole that accretes matter from the outer stellar envelope [77]. Another possible central engine may be a neutron star with a very strong magnetic field of about 10^{15} G, rotating with a millisecond period. Such a magnetar has a rotational energy $\sim 3 \times 10^{52}$ erg and can generate a power $> 10^{50}$ erg s^{-1} [119]. The stellar metallicity and the total duration of the central engine activity for a fixed value of the total energy release [120] can play a significant role in the formation of a relativistic jet with a Lorentz factor greater than 100, which is required to power a GRB. Collapsed stars are likely sources of long GRBs (type II in Fig. 8). However, these models meet with difficulty when trying to reproduce the features of short/hard (type I) GRBs. The type-I and type-II GRB populations are clearly separated in Fig. 8, suggesting their different origins. The LIGO/Virgo detection of gravitational radiation from GW 170817 associated with the short GRB 170817A [101, 103] confirmed the hypothesis [96] of the origin of short GRBs from binary neutron star coalescences [121]. Multiwavelength observations of GRB 170817A in the range from radio to gamma rays 160–200 days after the burst [122] impose some constraints on the models of relativistic outflows in GRBs.

The structure of relativistic outflows depends on both the energy release by the central engine and the mass and energy distribution around the source. The coalescence of two neutron stars is accompanied by their tidal destruction and strong heating of dense matter, which cools by neutrino emission. The wind accelerated by neutrinos sweeps out a cavern around the central source the cavern expands with a mildly relativistic velocity and a strongly anisotropic electromagnetic flux from the central source can propagate through it (see, e.g., [123]). The breakout of the cavern and the strongly collimated jet is accompanied by a short GRB with a characteristic light curve similar to the observed one.

In the case of a collapsed star, the collimated relativistic jet from the central source should propagate through the outer stellar envelope. Therefore, the energy of the collimated relativistic jet and of the accompanying mildly relativistic outflow with a wider opening angle on the stellar surface are determined by the structure of the outer layers and hence by the mass of the star and its metallicity. Observations suggest a possible relation between long GRBs and Wolf–Ryet stars — the progenitors of type-Ibc supernovae, in which relativistic velocity of the ejecta can be present [124].

Cosmological GRBs can be produced by Population-III stars with a high mass and low metallicity and, possibly, large mass of the collapsing core. The GRB detection rate estimated from the KONUS–WIND experiment as a func-

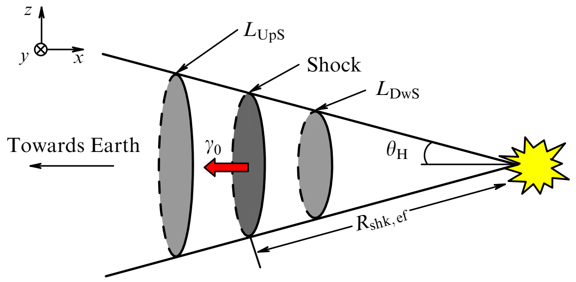

Figure 13. Relativistic shock propagation initiated by GRB ejecta into the circumstellar medium [138]. The model enables calculations of accelerated particle and energy emission spectra in the afterglow stage presented in Fig. 14.

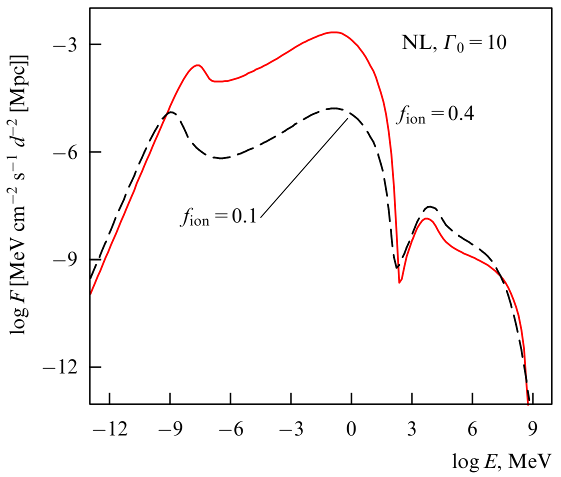

Figure 14. (Color online.) Model afterglow spectrum of a GRB [138]. The distributions of radiating particles accelerated by a relativistic shock with the initial Lorentz factor $\Gamma_0 = 10$ are calculated by a nonlinear Monte Carlo method. The shock propagation geometry is shown in Fig. 13.

tion of redshift up to $z \sim 5$, shown in Fig. 11, can be used to probe theoretical models proposed in [125, 126].

The breakout of the relativistic jet from the stellar surface must be accompanied by particle acceleration and the formation of nonthermal radiation spectra. The acceleration mechanism should provide an effective conversion of the relativistic outflow energy into accelerated particles [40, 41]. The modeling of relativistic jets from the central source typically involves the assumption of an initially highly magnetized plasma (see, e.g., [127, 128]). There is a problem of conversion of the jet magnetic field energy into the kinetic energy of the outflow or directly into accelerated particles by the magnetic reconnection process [129–131]. Extended particle energy distributions with hard tails, typical of GRB spectra (Band spectrum), can be produced by the Fermi acceleration mechanism at the site of internal shock collisions inside a dissipative relativistic outflow. A feature of the Fermi acceleration of particles by relativistic outflows with magnetic fluctuations is that the particle energy strongly changes in a single scattering, which requires going beyond the standard Fokker–Planck approximation [134, 135]. The formation of the hard spectrum of accelerated leptons $\propto p^{-\alpha}$ (where p is the particle momentum) with the exponent $\alpha \sim 1$, responsible for the rapid stage of the burst, is possible both in relativistic outflows with strongly magnetized inhomogeneous plasma and in low-magnetized flows [136, 137]. Furthermore, at the stage of expansion of the energy ejected by the central source into the circumstellar medium observed as GRB afterglow, relativistic shocks propagate in the nonmagnetized plasma (Fig. 13) and can accelerate cosmic rays to ultra-high energies [67, 136, 138, 139].

Modeling the afterglow radiation spectra requires the complex calculation of the shock front microstructure and the macroscopic downstream MHD flow, including the interaction of the energetic ejecta, which are possibly initially composed of magnetized electron–positron plasma with the nonmagnetized electron–ion plasma. The full modeling requires kinetic calculations in a wide dynamic range, which is unavailable with modern computers. The nonthermal afterglow spectra presented in Fig. 14 were calculated in [138] using a simplified model in which the relativistic shock is formed and propagates in the circumstellar electron–ion plasma. The model parameter is the ion energy fraction $f_{\rm ion}$ transferred to electrons and positrons during their first shock crossing. The accelerated particle distribution is calculated by a nonlinear Monte Carlo method taking the back reaction of the accelerated particles on the shock front structure into account. The broadband optical-to-gamma-ray photon spectra significantly depend on the model parameter $f_{\rm ion}$ characterizing the efficiency of the injection of electrons.

5. Prospects of studies of gamma-ray bursts and soft gamma-ray repeaters

Studies of GRBs and other cosmic transients related to catastrophic stellar core collapses, coalescences of neutron stars and black holes in binary systems, tidal disruptions of stars by massive black holes or of rapid magnetic energy transformations into radiation in SGRs have been included in the observational programs of large telescopes across the electromagnetic spectrum, neutrino telescopes, and gravitational-wave detectors.

GRBs, being the brightest explosions in the Universe, are observed from cosmological distances up to $z \sim 10$ and offer a unique tool for studying the early Universe and its evolution. In this respect, there are high hopes of the possible detection of high-redshift GRBs in the IR range using the forthcoming James Webb Space Telescope (JWST).

For closer GRBs at $z \lesssim 1$, future detection is expected of gravitational waves from coalescences of two neutron stars or of a neutron star and black hole by next-generation instruments, including the Einstein gravitational telescope (ET) [140] and Cosmic Explorer [141], which are planned to start operating after 2030. These instruments are ground-based laser interferometers with an arm length of $\sim 10-40$ km providing the capacity to measure gravitational wave polarization. The Advanced LIGO observatory that started a new science run in April 2019 has a detection horizon for binary neutron star coalescences of around 200 Mpc, which makes it possible to detect up to several dozen events like GW 170817 per year. For simultaneous observations of these events in the hard X-ray and gamma-ray range, wide-field detectors are needed that would be able to rapidly search for the localization region of a gravitational-wave event and to identify the possible electromagnetic counterpart.

Presently, two specialized space missions for observations of GRBs and other transients are planned: SVOM [142] and THESEUS [143, 144]. It is assumed that both missions will be equipped with several instruments covering the spectral range from optical to gamma rays (up to $\sim 5-20$ MeV). They will have a wide field of view (2π sr, the ECLAIR telescope for SVOM and XGIS instrument for THESEUS) and will be able to localize soft X-ray sources with an accuracy of better than 10 arcmin. These instruments will be able to both identify gravitational-wave sources and, thanks to the low (of the order of several keV) energy threshold of the main detectors, register GRBs from distances of up to $z \sim 10$, which will significantly increase our knowledge about the early Universe.

Probably, further progress in the understanding of the nature of magnetars, including generation mechanisms of giant magnetic fields and their 'genetic' relation to other classes of neutron stars, will be related to discoveries of new classes of magnetars and SGRs by the forthcoming wide-field instruments with a higher soft X-ray sensitivity (eXTP [145], THESEUS [143]). For known objects, prospects are related to X-ray polarimetric observations to recover the magnetic field geometry. Multiwavelength observations of pulsar wind nebulae can help to trace their activity history. The connection of magnetars with fast radio bursts (FRBs) is also very likely (see review [146]).

Studies of cosmic GRBs and SGRs at the Ioffe Institute will be continued with the new Spektr-UF (Konus-UF experiment) and Interhelioprobe (HELICON-I experiment) projects. Both instruments, owing to the observatory orbits, will continuously observe the entire sky and provide detailed measurements of temporal and spectral characteristics of GRBs, SGRs, solar flares, and other transients in the broad energy range 8 keV–15 MeV. A high time resolution in combination with a significant distance from Earth will enable the high-accuracy localization of short GRBs by the triangulation method for their reliable identification with gravitational-wave bursts.

The Ioffe Institute continues to develop sensitive silicon detectors for high-energy observations of transient sources in the framework of the ALEGRO [147] and eASTROGAM [148] international projects. The ground-based high-altitude Cherenkov telescope ALEGRO is designed for high-sensitivity observations of photons with energies above several GeV, i.e., the lowest energy available for atmospheric Cherenkov telescopes.

The eASTROGAM observatory [148], in addition to high-sensitivity MeV–GeV observations of GRB afterglows, will enable gamma-ray polarization measurements, which is significant for understanding radiation mechanisms.

The authors thank the referee, K A Postnov, for the useful remarks. The work of R L A, D D F, D S S, M V U, A E Ts, A V K, and A L L on studies of GRBs and other transients in the KONUS–WIND experiment is supported by the RSF grant 17-12-01378. The work of A M B on modeling astrophysical processes with extreme electromagnetic energy fluxes is supported by the RSF grant 16-12-10225.

Notes added in proofs

Observations and models of GRBs have not so far solved several fundamental problems, including the nature of their emission mechanisms and the magnetic field values both in the region of the GRB and in the afterglow formation region [149, 150]. Of special importance for the origin of the central engine is the GRB radiation mechanism. High-sensitivity observations by the KONUS–WIND, Fermi–GBM, Swift–BAT, and other detectors measured 15–150 keV spectra of a large sample of GRBs. At the same time, measurements of the proper GRB emission below 15 keV have been performed only for several dozen GRBs.

The 0.5–150 keV spectra were measured only for a small sample of GRBs observed by both Swift–BAT and Swift–XRT telescopes [151–153].

GRB models assuming the synchrotron emission mechanism from nonthermal accelerated electrons and positrons predict a photon spectrum consisting of several power-law parts (approximated by the law $\mathrm{d}F/\mathrm{d}E \sim E^{\Gamma}$) and, correspondingly, several spectral breaks. The spectrum evolves with time; therefore, a comparison with observational data requires taking the time resolution of the detectors into account and simultaneous observations by several detectors. At the lowest energies, the spectral breaks can correspond to the transition from the synchrotron self-absorption (with the photon index $\Gamma = 1$) to the spectrum with the photon index $\Gamma = -2/3$ corresponding to the emission from electrons and positrons with an energy close to the minimal energy of the nonthermal distribution. At higher energies, the spectral shape depends on the efficiency of synchrotron and Compton energy losses by leptons. In the fast cooling regime, nonthermal particles lose most of the energy to emission inside the source volume. Otherwise, slow cooling occurs (or the intermediate case of moderate cooling). For a power-law distribution of nonthermal electrons in the source ($\mathrm{d}N/\mathrm{d}E \sim E^{-s}$), the photon radiation indexes are $\Gamma = -(s+2)/2$ and $\Gamma = -(s+1)/2$ for the respective fast and slow cooling. During the GRB prompt emission phase, the existing models of acceleration of nonthermal particles predict spectra of leptons accelerated by strong turbulence with indexes $s = 1$ up to some maximum energy [134]. During the afterglow stage, the photon index is predicted to be $s > 2$ [41].

In the emission spectra of 8 out of 10 long GRBs, the authors of [152] discovered a spectral break at low energies. Photon indexes below the break obtained in [151, 152] are consistent with the expected value $\Gamma = -2/3$ in the synchrotron model below the spectral break. Above the spectral break but below the photon energies corresponding to the Band function peak, the photon index was found to be $\Gamma = -3/2$. The break was not discovered in the short GRBs that have been analyzed. However, their photon index below the peak was found to be very hard and consistent with $\Gamma = -2/3$. The study of GRB spectra taking their soft X-ray emission into account made it possible to discover spectral breaks and supported the model of synchrotron emission with moderate cooling of radiating leptons. Nor do the 0.5–150 keV observations contradict a combined model with a black-body photospheric emission and nonthermal power-law radiation at high energies. For a limited sample of several GRBs, the prompt optical emission with the time variability typical for GRBs was observed [153]. In these GRBs, the synchrotron radiation from nonthermal particles with power-law distributions can explain the observations, while the simple one-zone model with a black-body component is inconsistent with the data. To make the model consistent with observations, additional spectral breaks should be involved, which is difficult to justify. The authors of [151–153] noted that the interpretation of their observations by the standard models assumes a magnetic field less than 100 G inside the GRB (in the comoving frame), which is by orders of magnitude smaller than have been assumed up to now.

So far, only the first results about the proper GRB emission spectra with good time resolution have been obtained, which has already demonstrated the possibility of detailed tests of the emission and particle acceleration models in GRBs. As noted above, the time-resolved polarization measurements of proper GRB emission jointly with broadband spectral data allow testing the models of synchrotron components in GRB radiation [154].

References

1. Klebesadel R W, Strong I B, Olson R A *Astrophys. J.* **182** L85 (1973)
2. Golenetskii S V et al. *Prib. Tekh. Eksp.* (4) 203 (1969)
3. Golenetskii S V, Mazets E P *JETP Lett.* **14** 131 (1971); *Pis'ma Zh. Eksp. Teor. Fiz.* **14** 201 (1971)
4. Golenetskii S V et al. *Astrophys. Lett.* **9** 69 (1971)
5. Mazets E P, Golenetskii S V, Il'inskii V N *JETP Lett.* **19** 77 (1971); *Pis'ma Zh. Eksp. Teor. Fiz.* **19** 126 (1971)
6. Golenetskii S V, Il'inskii V N, Mazets E P *Cosmic Res.* **12** 706 (1974); *Kosm. Issled.* **12** 779 (1974)
7. Mazets E P et al. *AIP Conf. Proc.* **101** 36 (1983)
8. Mazets E P et al. *Astrophys. Space Sci.* **80** 3 (1981)
9. Golenetskii S V et al. *Nature* **306** 451 (1983)
10. Kouveliotou C et al. *Astrophys. J.* **413** L101 (1993)
11. Band D et al. *Astrophys. J.* **413** 281 (1993)
12. Aptekar R L et al. *Space Sci. Rev.* **71** 265 (1995)
13. Mazets E P et al. *Nature* **282** 587 (1979)
14. Evans W D et al. *Astrophys. J.* **237** L7 (1980)
15. Cline T L et al. *Astrophys. J.* **237** L1 (1980)
16. Cline T L et al. *Astrophys. J.* **255** L45 (1982)
17. Barat C et al. *Astron. Astrophys.* **79** L24 (1979)
18. Mazets E P, Golenetskii S V, Gur'yan Y A *Sov. Astron. Lett.* **5** 641 (1979); *Pis'ma Astron. Zh.* **5** 641 (1979)
19. Laros J G et al. *Astrophys. J.* **320** L111 (1987)
20. Kouveliotou C et al. *Astrophys. J.* **322** L21 (1987)
21. Kuiper L et al. *Astrophys. J.* **645** 556 (2006)
22. Kaspi V M, Beloborodov A M *Annu. Rev. Astron. Astrophys.* **55** 261 (2017)
23. Mereghetti S, Pons J A, Melatos A *Space Sci. Rev.* **191** 315 (2015)
24. Mazets E P et al. *Astron. Lett.* **25** 635 (1999); *Pis'ma Astron. Zh.* **25** 735 (1999)
25. Frederiks D D et al. *Astron. Lett.* **33** 1 (2007); *Pis'ma Astron. Zh.* **33** 3 (2007)
26. Mazets E P et al. *Astrophys. J.* **680** 545 (2008)
27. Mazets E P, Golenetskii S V *Astrophys. Space Sci.* **75** 47 (1981)
28. Mazets E P et al. *Astrophys. Space Sci.* **84** 173 (1982)
29. Hurley K *Adv. Space Res.* **47** 1337 (2011)
30. Svinkin D S et al. *Mon. Not. R. Astron. Soc.* **447** 1028 (2015)
31. Frederiks D D et al. *Astron. Lett.* **33** 19 (2007); *Pis'ma Astron. Zh.* **33** 22 (2007)
32. Svinkin D S et al. *Astrophys. J. Suppl.* **224** 10 (2016)
33. Duncan R C, Thompson C *Astrophys. J.* **392** L9 (1992)
34. Thompson C, Duncan R C *Mon. Not. R. Astron. Soc.* **275** 255 (1995)
35. Kouveliotou C et al. *Nature* **393** 235 (1998)
36. Fishman G J et al. *Astrophys. J. Suppl.* **92** 229 (1994)
37. Costa E et al. *Nature* **387** 783 (1997)
38. van Paradijs J et al. *Nature* **386** 686 (1997)
39. Bloom J S et al. *Astrophys. J.* **507** L25 (1998)
40. Mészáros P *Annu. Rev. Astron. Astrophys.* **40** 137 (2002)
41. Piran T *Rev. Mod. Phys.* **76** 4 1143 (2004)
42. Gehrels N, Ramirez-Ruiz E, Fox D B *Annu. Rev. Astron. Astrophys.* **47** 567 (2009)
43. Willingale R, Mészáros P *Space Sci. Rev.* **207** 63 (2017)
44. Metzger M R et al. *Nature* **387** 878 (1997)
45. Gehrels N et al. *Astrophys. J.* **611** 1005 (2004)
46. Gehrels N et al. *Nature* **437** 851 (2005)
47. Meegan C et al. *Astrophys. J.* **702** 791 (2009)
48. Atwood W B et al. *Astrophys. J.* **697** 1071 (2009)
49. Ackermann M et al. *Science* **343** 42 (2014)
50. Tsvetkova A et al. *Astrophys. J.* **850** 161 (2017)
51. Pal'shin V D et al. *Astrophys. J. Suppl.* **207** 38 (2013)
52. Hurley K et al. *Astrophys. J. Suppl.* **207** 39 (2013)
53. Lipunov V M *Astron. Astrophys. Trans.* **29** 143 (2016)
54. Singer L P et al. *Astrophys. J.* **806** 52 (2015)
55. Bellm E, in *The Third Hot-Wiring the Transient Universe Workshop, HTU-III, 13 – 15 November, 2013, Santa Fe, NM* (Eds P R Wozniak et al.) p. 27
56. Aptekar R L et al. *Phys. Usp.* **53** 401 (2010); *Usp. Fiz. Nauk* **180** 420 (2010)
57. Levan A J et al. *Astrophys. J.* **781** 13 (2014)
58. Evans P A et al. *Mon. Not. R. Astron. Soc.* **444** 250 (2014)
59. Frederiks D D et al. *Astrophys. J.* **779** 151 (2013)
60. Greiner J et al. *Astron. Astrophys.* **498** 89 (2009)
61. Atteia J et al. *Astrophys. J.* **837** 119 (2017)
62. Stanek K Z et al. *Astrophys. J.* **522** L39 (1999)
63. Galama T J et al. *Nature* **395** 670 (1998)
64. Iwamoto K et al. *Nature* **395** 672 (1998)
65. Cano Z et al. *Adv. Astron.* **2017** 8929054 (2017)
66. Soderberg A M et al. *Nature* **463** 513 (2010)
67. Bykov A M *Phys. Usp.* **61** 805 (2018); *Usp. Fiz. Nauk* **188** 894 (2018)
68. Kann D A et al. *Astron. Astrophys.* **624** A143 (2019)
69. Woosley S E, Eastman R G, Schmidt B P *Astrophys. J.* **516** 788 (1999)
70. Woosley S E, Heger A *Astrophys. J.* **752** 32 (2012)
71. Lipunov V M, Postnov K A, Prokhorov M E *Astron. Rep.* **45** 236 (2001); *Astron. Zh.* **78** 276 (2001)
72. Atteia J *Astron. Astrophys.* **328** L21 (1997)
73. Friedman A S, Bloom J S *Astrophys. J.* **627** 1 (2005)
74. Amati L et al. *Astron. Astrophys.* **390** 81 (2002)
75. Yonetoku D et al. *Astrophys. J.* **609** 935 (2004)
76. Ghirlanda G, Ghisellini G, Lazzati D *Astrophys. J.* **616** 331 (2004)
77. MacFadyen A I, Woosley S E *Astrophys. J.* **524** 262 (1999)
78. Hopkins A M *Astrophys. J.* **615** 209 (2004)
79. Bouwens R J et al. *Nature* **469** 504 (2011)
80. Hanish D J et al. *Astrophys. J.* **649** 150 (2006)
81. Thompson R I et al. *Astrophys. J.* **647** 787 (2006)
82. Li L-ñ *Mon. Not. R. Astron. Soc.* **388** 1487 (2008)
83. Komissarov S S, Barkov M V *Mon. Not. R. Astron. Soc.* **402** L25 (2010)
84. de Souza R S, Yoshida N, Ioka K *Astron. Astrophys.* **533** A32 (2011)
85. Tanvir N R et al. *Mon. Not. R. Astron. Soc.* **483** 5380 (2019)
86. Petitjean P et al. *Space Sci. Rev.* **202** 195 (2016)
87. Ackermann M et al. *Astrophys. J.* **716** 1178 (2010)
88. Amelino-Camelia G et al. *Nature* **393** 763 (1998)
89. Abdo A A et al. *Nature* **462** 331 (2009)
90. Vestrand W T et al. *Nature* **442** 172 (2006)
91. Racusin J L et al. *Nature* **455** 183 (2008)
92. Gao H, Wu X-F, Mészáros P *Astrophys. J.* **810** 121 (2015)
93. Hulse R A, Taylor J H *Astrophys. J.* **195** L51 (1975)
94. Blinnikov S I et al. *Sov. Astron. Lett.* **10** 177 (1984); *Pis'ma Astron. Zh.* **10** 422 (1984)
95. Paczynski B *Astrophys. J.* **308** L43 (1986)
96. Eichler D et al. *Nature* **340** 126 (1989)
97. Narayan R, Paczynski B, Piran T *Astrophys. J.* **395** L83 (1992)
98. Abramovici A et al. *Science* **256** 325 (1992)
99. Lattimer J M et al. *Astrophys. J.* **213** 225 (1977)
100. Berger E *Annu. Rev. Astron. Astrophys.* **52** 43 (2014)
101. Abbott B P et al. *Astrophys. J.* **848** L12 (2017)
102. Svinkin D et al. *GCN Circ.* (21515) (2017); https://gcn.gsfc.nasa.gov/gcn3/21515.gcn3
103. Abbott B P et al. *Astrophys. J.* **848** L13 (2017)
104. D'Avanzo P et al. *Astron. Astrophys.* **613** L1 (2018)
105. Mooley K P et al. *Nature* **561** 355 (2018)
106. Mooley K P et al. *Astrophys. J. Lett.* **868** L11 (2018)
107. Blanchard P K et al. *Astrophys. J.* **848** L22 (2017)
108. Cowperthwaite P S et al. *Astrophys. J.* **848** L17 (2017)
109. Nicholl M et al. *Astrophys. J.* **848** L18 (2017)
110. Kasen D et al. *Nature* **551** 80 (2017)
111. Burenin R A *Astron. Lett.* **26** 269 (2000); *Pis'ma Astron. Zh.* **26** 323 (2000)
112. Frederiks D D et al., in *Third Rome Workshop on Gamma-Ray Bursts in the Afterglow Era. Proc. of the Conf., 17 – 20 September 2002, Rome, Italy* (ASP Conf. Series, Vol. 312, Eds M Feroci et al.) (San Francisco: Astronomical Society of the Pacific, 2004) p. 197
113. Norris J P, Bonnell J T *Astrophys. J.* **643** 266 (2006)

114. Cavallo G, Rees M J *Mon. Not. R. Astron. Soc.* **183** 359 (1978)
115. Goodman J *Astrophys. J.* **308** L47 (1986)
116. Shemi A, Piran T *Astrophys. J.* **365** L55 (1990)
117. Rees M J, Mészáros P *Astrophys. J.* **430** L93 (1994)
118. Woosley S E, Bloom J S *Annu. Rev. Astron. Astrophys.* **44** 507 (2006)
119. Woosley S, in *Gamma-Ray Bursts* (Cambridge Astrophysics Series, Vol. 51, Eds C Kouveliotou, R A M J Wijers, S Woosley) (Cambridge: Cambridge Univ. Press, 2012)
120. Lazzati D et al. *Astrophys. J.* **750** 68 (2012)
121. Kasliwal M M et al. *Science* **358** 1559 (2017)
122. Margutti R et al. *Astrophys. J.* **848** L20 (2017)
123. Bromberg O et al. *Mon. Not. R. Astron. Soc.* **475** 2971 (2018)
124. Soderberg A M et al. *Nature* **453** 469 (2008)
125. Suwa Y, Ioka K *Astrophys. J.* **726** 107 (2011)
126. Aloy M A, Cuesta-Martínez C, Obergaulinger M *Mon. Not. R. Astron. Soc.* **478** 3576 (2018)
127. Lyutikov M *New J. Phys.* **8** 119 (2006)
128. Granot J et al. *Space Sci. Rev.* **191** 471 (2015)
129. Zhang B, Yan H *Astrophys. J.* **726** 90 (2011)
130. Kagan D et al. *Space Sci. Rev.* **191** 545 (2015)
131. Lemoine M, Pelletier G *Comptes Rendus Phys.* **16** 628 (2015)
132. Uzdensky D A, in *Magnetic Reconnection: Concepts and Applications* (Astrophysics and Space Science Library, Vol. 427, Eds W Gonzalez, E Parker) (Switzerland: Springer, 2016) p. 473
133. Blandford R et al. *Space Sci. Rev.* **207** 291 (2017)
134. Bykov A M, Meszaros P *Astrophys. J.* **461** L37 (1996)
135. Bykov A et al. *Space Sci. Rev.* **173** 309 (2012)
136. Xu S, Yang Y, Zhang B *Astrophys. J.* **853** 43 (2018)
137. Lemoine M, Waxman E *J. Cosmol. Astropart. Phys.* **11** 009 (2009)
138. Warren D C et al. *Mon. Not. R. Astron. Soc.* **452** 431 (2015)
139. Bykov A M et al. *Space Sci. Rev.* **214** 41 (2018)
140. Sathyaprakash B et al. *Class. Quantum Grav.* **29** 124013 (2012)
141. LIGO Scientific Collab. Technical Note, LIGO-T1700231 (2017), https://dcc.ligo.org/LIGO-T1700231/public
142. Cordier B et al., arXiv:1512.03323
143. Amati L et al. *Adv. Space Res.* **62** 191 (2018)
144. Stratta G et al. *Adv. Space Res.* **62** 662 (2018)
145. Zhang S N et al. *Proc SPIE* **9905** 99051Q (2016)
146. Popov S B, Postnov K A, Pshirkov M S *Phys. Usp.* **61** 965 (2018); *Usp. Fiz. Nauk* **188** 1063 (2018)
147. Bykov A M et al. *Tech. Phys.* **62** 819 (2017); *Zh. Tekh. Fiz.* **87** 803 (2017)
148. De Angelis A et al. (The e-ASTROGAM Collab.) *Exp. Astron.* **44** 25 (2017)
149. Mészáros P *Annu. Rev. Nucl. Part. Sci.* **67** 45 (2015)
150. Božnjak Ž, Daigne F *Astron. Astrophys.* **568** A45 (2014)
151. Oganesyan G et al. *Astron. Astrophys.* **616** A138 (2018)
152. Ravasio M E et al. *Astron. Astrophys.* **625** A60 (2019)
153. Oganesyan G et al. *Astron. Astrophys.* **628** A59 (2019)
154. De Angelis A et al. *J. High Energy Astrophys.* **19** 1 (2018)